journal

J. Am. Ceram. Soc., 73 [10] 2848–56 (1990)

Structure of Sodium Aluminosilicate Glasses

David M. Zirl* and Stephen H. Garofalini*

Department of Ceramics, Rutgers University, Piscataway, New Jersey 08855-0909

A series of sodium aluminosilicate glasses composed of varying ratios (R) of Al_2O_3/Na_2O ($0.25 \leq R \leq 2.0$) has been simulated with the molecular dynamics technique using a tetrahedral form of a three-body interaction potential. Extrema in the activation energies for sodium diffusion and in the diffusion constants for all of the atomic species were observed for glasses with equal concentrations of Al_2O_3 and Na_2O ($R = 1.0$). These changes corresponded to the minimum observed experimentally in the activation energy for electrical conductivity and to the maximum observed in the viscosity for glasses with compositions of $R = 1.0$. The coordination of aluminum remained 4 over the entire compositional range, negating the need to invoke a coordination change of aluminum to explain the changes in the physical properties. The changes to the simulated physical properties as R passed through the equivalence point were attributed to the elimination of nonbridging oxygen, to the introduction of oxygen triclusters, and to changes in the distribution of ring structures within the glass networks. [Key words: sodium, aluminosilicates, molecular dynamics, glass, structure.]

I. Introduction

EXTREMA occur in the viscosity and electrical conductivity of sodium aluminosilicate (NAS) glasses as the ratio of aluminum to sodium (R = Al/Na) passes through the equivalence point.[1–9] The observed changes in the properties of the series of glasses with compositions of $R = 1$ are believed to be due to structural changes within the glass network. Several structural models have been proposed to explain these physical changes. These models assume similar chemical environments and structural roles for the sodium. In glasses with compositions of $R < 1$ sodium either coordinates nonbridging oxygen (NBO) or charge compensates aluminate tetrahedra, while in glasses with compositions of $R \geq 1$ the NBO disappears and the sodium acts only as a charge compensator.

The proposed models are the following: (a) The coordination of Al changes from being tetrahedral to being both tetrahedral and octahedral as R passes through the equivalence point.[1–8] In compositions with $R \leq 1$, the aluminum acts as network formers and replaces the silicon in the network. The aluminate tetrahedra $[AlO_4]^-$ are charge compensated by the sodium. In glasses with the composition of $R > 1$ there no longer exists enough excess sodium to charge compensate the aluminate tetrahedra, so some of the aluminum changes from being tetrahedrally coordinated, like the network-forming silicon, to being octahedrally coordinated, like the network-modifying sodium. Riebling, using viscosity measurements and molar volume calculations, proposed that 1/4 of the aluminum in excess of the sodium becomes octahedrally coordinated.[5] The changes in the physical properties (viscosity, electrical conductivity) could be associated with the change in aluminum coordination and with the removal of the singly bound oxygen.

(b) Alternatively, aluminum remains tetrahedrally coordinated over the entire compositional range and changes to the network topology (ring connectivity), to the bond angles within the glasses (Si–O–Si or Si–O–Al), or the introduction of triclusters could account for the physical property changes.[9,10] Triclusters are composed of three tetrahedra which meet at a common vertex to form a three-coordinated oxygen.[9]

Raman spectroscopy,[10a] EXAFS (extended X-ray absorption fine structure) and XANES (X-ray absorption near edge structure),[10b,c] and energy dispersive X-ray diffraction[10d] performed on a series of NAS glasses showed that Al remained four-coordinated over the whole compositional range ($0 < R < 1.61$) and that as the ratio of Al/Na was increased there was an increase in the degree of polymerization of the network. The property changes in glasses with compositions of $R \geq 1$ were thought to be associated with the cross-linking of rings within the network which would cause smaller rings to occur and make the diffusivity of the sodium more difficult (i.e., Na conductivity decreased through channels in glass). Changes to the bond angles could lead to a puckering of the network which in turn would also alter the sodium diffusivity.

The argument for tricluster formation was based upon the geometrical packing of oxygen around aluminum and on the oxygen density necessary for octahedra to form.[9] Triclusters have been presumed in calcium aluminosilicate glasses when there was excess aluminum present in the glass.[11] Triclusters are found in crystalline mullite ($2Al_2O_3 \cdot 3SiO_2$) which can be considered an "end" member to the NAS glass composition ($R \rightarrow \infty$, as concentration of Na goes to zero).

The competing models have received considerable attention both experimentally and theoretically. The traditional view of a change in Al coordination is a convenient way to explain the anomalies in the physical properties. However, the only evidence for the change in Al coordination has been inferred from Al$K\alpha$ X-ray emission.[3c] Rindone and associates used X-ray fluorescence (XRF) to compare structural units in NAS glasses to those in Al_2O_3 and Al metals. They found slight shifts in the Al$K\alpha$ spectra away from four-coordination in glasses with compositions of $R \geq 1$ and attributed these shifts to the presence of aluminum in octahedral configurations. These shifts, however, could be associated with the instability in the glasses with compositions of $R > 1$ as these glasses show tendencies toward phase separation. Infrared spectroscopic evaluation of NAS by the same research group, however, did not confirm the existence of the octahedrally coordinated aluminum.[3b,e] A more recent XRF study on NAS glasses formed using rf sputtering techniques showed shifts (<11%) away from the tetrahedrally coordinated aluminum, in the Al$K\alpha$ emission spectra of the NAS glasses which could have been caused by the existence of the over-coordinated aluminum.[12]

J. Shelby—contributing editor

Manuscript No. 197804. Received January 30, 1990; approved May 27, 1990.

Presented at the 92nd Annual Meeting of the American Ceramic Society, Dallas, TX, April 23, 1990 (Glass Division, Paper No. 2-G-90).

Supported by the Department of Energy under Contract No. DE-FG05-88ER45368 and by the Fiber Optic Materials Research Program at Rutgers University.

*Member, American Ceramic Society.

Octahedrally coordinated aluminum has been shown to exist in glasses under extremely high pressures.[13,14] NMR studies of albite glass ($NaAlSi_3O_8$) at pressures less than 30 kbar (3 GPa) found Al^{3+} to be tetrahedrally coordinated, while at pressures around 80 kbar (8 GPa) Al^{3+} was octahedrally coordinated.[14] These changes in coordination with pressure have also been studied in molecular dynamic (MD) simulations of aluminosilicates.[14]

X-ray photoelectron spectroscopy (XPS) has also been used to study a series of NAS glasses.[15-18] The O 1*s* signals were resolved into contributions from bridging and nonbridging oxygen. It was proposed that six-coordinated Al formed at $R > 0.7$ to 0.8 based upon the disappearance of the NBO O 1*s* signal at $R = 0.7$ to 0.8.[15,16] However, Onorato *et al.*[19,20] using a Au-calibration technique analyzed NAS fracture surfaces and found that the NBO signal vanished at $R = 1.0$. The Au-calibration technique allowed for the XPS signals to be referenced to the Fermi level of the insulator instead of to some arbitrary peak (Si 2*p*) which may have been affected by excessive charging. Additionally, Tl^+ probe luminescence[21-23] confirmed the existence of the NBO up to the equivalence point and refuted the notion of octahedrally coordinated Al below the equivalence point consuming NBO.[15-18]

The MD technique has been used to model silica and silicate glasses.[24-26] The resulting structures have compared favorably with experimentally derived bond distances, bond angle distributions, coordination numbers, concentration and types of defects, static structure factors, and distribution of Q species[27] for both the silica and sodium silicate glasses. MD simulations allow for determination of coordination environments around specific atom types and can be used to study diffusion at "high" temperatures.[28-31] Recent simulations employing multibody potentials[25,26] have shown that bond directionality, which exists in the partially covalent silicate systems, can be incorporated into the calculations. The multibody interatomic potentials energetically penalized the systems for deviations from a given critical angle and the resultant structures for silica and silicate glasses showed a nearly perfect tetrahedral coordination environment around the silicon, and much narrower tetrahedral and siloxane bond angle distributions than had been determined for glasses created using only pair potentials.

In this present study a tetrahedral form of the three-body potential was applied to Si, O, and Al as the central atoms in atomic triplets, in order to test the hypothesis that the changes in the macroscopic properties of the NAS glasses can occur without changes occurring to the aluminum coordination. Tetrahedral coordination of the aluminum was energetically more favorable in the simulations and so by determining both the sodium diffusivity and the diffusivity of all of the species comparisons were made to experimentally determined activation energies for electrical conductivity and to viscosity measurements.

II. Experimental Procedure

Constant-volume MD simulations were used with a Nordsieck–Gear[32] type of algorithm to integrate Newton's classical equations of motion with a time step of integration of 0.001 ps. The total potential energy, V_t, acting on each atom in the system was composed of contributions from two- and three-body interactions:

$$V_t = V_2 + V_3 \tag{1}$$

The two-body potential was a modified Born–Mayer–Huggins type of potential, acting between atoms i and j, which were separated by distance r_{ij}. The potential had the functional form

$$V_2 = A_{ij} \exp(-r_{ij}/\rho_{ij}) + (q_i q_j/r_{ij}) \operatorname{erfc}(r_{ij}/\beta_{ij}) \tag{2}$$

The first term in Eq. (2) was due to short-range interactions and the second term was due to Coulombic interactions. The softness parameter, ρ_{ij}, was set to 0.29×10^{-8} cm for all interaction pairs and the parameters q_i, q_j, A_{ij}, and β_{ij} are presented in Table I.[25,26]

Table I. Parameters for Two-Body Potentials

Atom pair	A_{ij} ($\times 10^{-15}$ J)	β_{ij} ($\times 10^{-8}$ cm)
Si–Si	0.1877	0.230
Si–O	0.2962	0.234
Si–Al	0.2523	0.233
Si–Na	0.2001	0.230
O–O	0.0750	0.230
O–Al	0.2750	0.234
O–Na	0.3195	0.234
Al–Al	0.3418	0.235
Al–Na	0.2178	0.230
Na–Na	0.2159	0.230

The three-body contribution to the total potential energy was a Stillinger–Weber[33] type of potential developed by Feuston and Garofalini[25,26] for use in silica and silicate systems. The three-body potential, V_3, acted between atoms i, j, and k which met at a common vertex, i, subtended by angle θ_{jik}. The three-body contribution energetically penalized the system for deviations from an angle θ^c, when atoms j and k were within radial cutoff distances of r_i^c. The critical angle, θ^c, corresponded to the tetrahedral angle of 109.48°. Three-body contributions were imposed on all triplets involving Si, O, and Al as the central atoms and took the following functional form:

$$V_3 = \lambda_i \exp[(\gamma_i/(r_{ij} - r_i^c) + \gamma_i/(r_{ik} - r_i^c)] \times (\cos\theta_{jik} - \cos\theta^c)^2 \quad (\text{if } r_{ij} < r_i^c, \text{ and } r_{ik} < r_i^c) \tag{3a}$$

or

$$V_3 = 0 \quad (\text{if } r_{ij} \geq r_i^c \text{ or } r_{ik} \geq r_i^c) \tag{3b}$$

The values for parameters λ_i and γ_i are presented in Table II. The parameters were similar to those used in earlier simulations of silica and silicate glasses,[25,26] which had been determined by fit to experimental structural features such as radial distribution functions, bond angle distributions, and static structure factors. The three-body parameters on the Al were set equal to those on Si in order to bias the Al to tetrahedral coordination and evaluate the effect on physical properties. The three-body contributed less than 1% to the total potential energy of the vitreous silica system[25] as well as the NAS systems studied here, yet greatly improved the comparison between simulated and experimental structural features.

Four NAS glasses were simulated in the present study. The silica concentration in the glasses was kept at approximately 63% while the ratio (R) of Al_2O_3 to Na_2O was 0.25, 0.64, 1.0, and 2.0. The compositions and densities of the glasses studied and ratios of Al/Na and Al/Si are presented in Table III. The densities used here were taken from the experimental densities[8] (density at $R = 2.0$ extrapolated from experimental data up to $R = 1.7$).

The NAS glasses were formed using a simulated melt-quench technique which involved scaling the kinetic energy of the systems of atoms from elevated temperatures to room temperature. The quench sequence is presented in Table IV and involved a total time of approximately 350 ps (corresponding to 350 000 iterations). Velocity rescaling was performed every 10th move for approximately the first 8 to 10 ps

Table II. Parameters for Three-Body Potentials

	X–O–X*	O–Si–O	O–Al–O
r_i^c (Å)	2.6	3.0	3.0
λ_i ($\times 10^{-18}$ J)	1.0	24.0	24.0
γ_i (Å)	2.0	2.8	2.8

*X = Si, Al.

Table III. Compositions and Initial Properties of NAS Glasses

R(Al/Na)	*M*(Al/Si)	Density* (g/cm³)	No. of atoms	Empirical formula
0.25	0.25	2.489	369	$4Na_2O \cdot 1Al_2O_3 \cdot 8SiO_2$
0.64	0.46	2.477	362	$25Na_2O \cdot 16Al_2O_3 \cdot 69SiO_2$
1.00	0.57	2.465	370	$2Na_2O \cdot 2Al_2O_3 \cdot 7SiO_2$
2.00	0.84	2.452	327	$4Na_2O \cdot 8Al_2O_3 \cdot 19SiO_2$

*Reference 8.

at each temperature. The length of equilibration for each temperature is also shown in Table IV.

Three glasses were made at each of the four compositions through separate quench procedures. The first quench for each composition was held at 8000 K for 12 ps; the second series of quenches was started from the stored final configurations at 8000 K from the first series of quenches and run for an additional 15 ps before continuing with the quenching cycle (see Table IV). The third series of quenches was continued from the stored final configurations from the second quench series at 8000 K for an additional 20 ps prior to continuing with the quenching cycle (see Table IV). Statistics were gathered on the glasses at 300 K for all three series of quenches from additional 1-ps runs, where positions and velocities were saved every 10th iteration. Local and medium-range order in the glasses was determined as averages over each of the three quenches for each of the glass compositions.

Diffusion coefficients were computed from the mean squared displacement $l^2(\tau)$ between some position vector, $\mathbf{r}_i$, at some initial time ($\tau = 0$) and some later time ($\tau = \tau_0 + \Delta\tau$):

$$\langle l^2(\tau)\rangle_\alpha = (1/N_\alpha)\sum \langle |\mathbf{r}_i(\tau) - \mathbf{r}_i(\tau_0)|^2\rangle \quad (4)$$

where

$$D = (1/6)l^2/\tau \quad (5)$$

and N_α is the number of diffusing atoms. Activation energies were determined using the Arrhenius-type relationship

$$D = D_0 \exp(-Q/\mathrm{RT}) \quad (6)$$

where Q is the activation energy for diffusion, T is the temperature, and R is the gas constant. Diffusion statistics were gathered from additional 10-ps continuation runs at 6500, 6000, 5000, and 4000 K from two of the quench sequences.

The local atomic structure of the series of NAS glasses will be discussed in Section III(1), network connectivity will be discussed in Section III(2), and diffusivity and activation energies will be discussed in Section III(3).

III. Results and Discussion

(1) Local Structure

Local structure in glasses can be classified according to the bond lengths between atomic pairs and the coordination environments around individual atoms. Pair distribution functions (PDFs) for Si–O bonds for all four glasses are presented in Fig. 1(A). The PDFs are from one series of quenches which are representative of the structures found from all three quenches. The average Si–O bond lengths of 1.59 to 1.61 Å* correspond favorably to bond lengths derived from EXAFS and energy dispersive X-ray diffraction performed on NAS

Table IV. Quench Sequence for Series of Sodium Aluminosilicate Glasses

Temperature (K)	Time (ps)	Equilibration time (ps)
8000	*	8
7500	12	8
7000	15	8
6500	15	8
6000	15	8
5500	20	10
5000	30	10
4500	30	10
4000	40	10
3500	40	10
3000	20	10
2500	20	8
2000	15	8
1500	15	8
1000	15	8
300	15	8

*See text.

*1 Å = 0.1 nm.

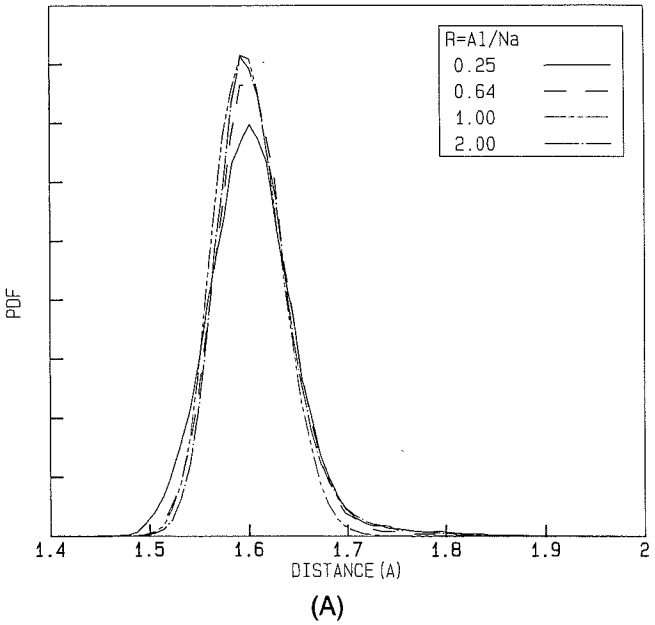

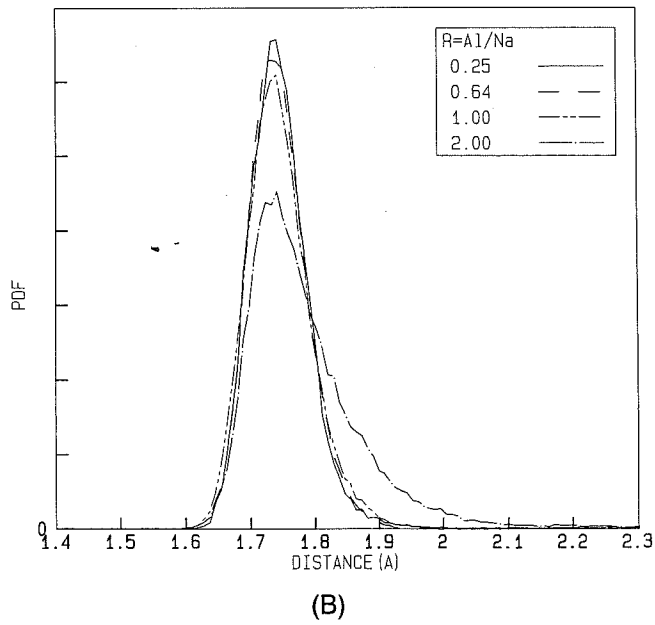

Fig. 1. Pair distribution functions plotted versus distance for (A) Si–O and (B) Al–O.

glasses and crystals.[10d,34] Coordination numbers can be determined by integrating the area under the major peak in the PDF (Fig. 1(A)). This can be facilitated by noting the plateau in the graph of coordination versus distance. An example of this type of plot is shown in Fig. 2(A) for the coordination environment of oxygen around silicon. The average coordination around the silicon was 4 for the entire series of glasses.

The PDFs and coordination environments of oxygen around Al are presented in Figs. 1(B) and 2(B). The average Al–O bond lengths of 1.74 to 1.75 Å compare favorably with Al–O bond lengths of 1.74 to 1.77 Å derived from an EXAFS study on NAS glasses,[10c] with the Al–O bond lengths in low albite, which is a crystalline analogue of the NAS glasses[35] and with bond lengths determined from molecular orbital calculations.[36] The coordination versus distance curves in Fig. 2(B) clearly show plateaus at four oxygens around aluminum for all of the compositions. The curve for $R = 2.0$ does not plateau at 4 until almost 2.1 Å, which can be attributed to the association of three-coordinated bridging oxygen (triclusters) with aluminate tetrahedra, as will be discussed below. Thus the aluminum remained four-coordinated over the entire compositional range.

Oxygen coordination plays an important role in the NAS series of glasses. NBO is oxygen bound to only one silicon. The concentration of NBO versus the glass composition is presented in Fig. 3 (solid curve), along with the theoretical concentration of NBO (dashed curve).[37] The concentration of NBO was reduced as aluminum was substituted for sodium. For the glasses with compositions of $R = 2$ less than 1% of all of the oxygen was singly bonded to silicon. The NBOs had sodium associated with them at all compositions, as will be discussed in the section on sodium coordination.

Increasing the concentration of aluminum also caused a transition in the types of the bridging oxygen (BO) in the glasses. BO was bonded to two cations which were either two silicons, one silicon and one aluminum, or two aluminums. The concentration of the type of BO versus the glass composition is presented in Fig. 4. The transition from a predominance of the Si–O–Si type of bond to a predominance of the Si–O–Al type of bond occurred at approximately $R = 1$, indicating that the aluminum was fully incorporated into the network.

The presence of Al–O–Al bonds in this study seems to be in violation of Lowenstein's aluminum avoidance principle,[38] which states that for two tetrahedrons joined by a BO, only one of the cations in the center of the tetrahedra can be an

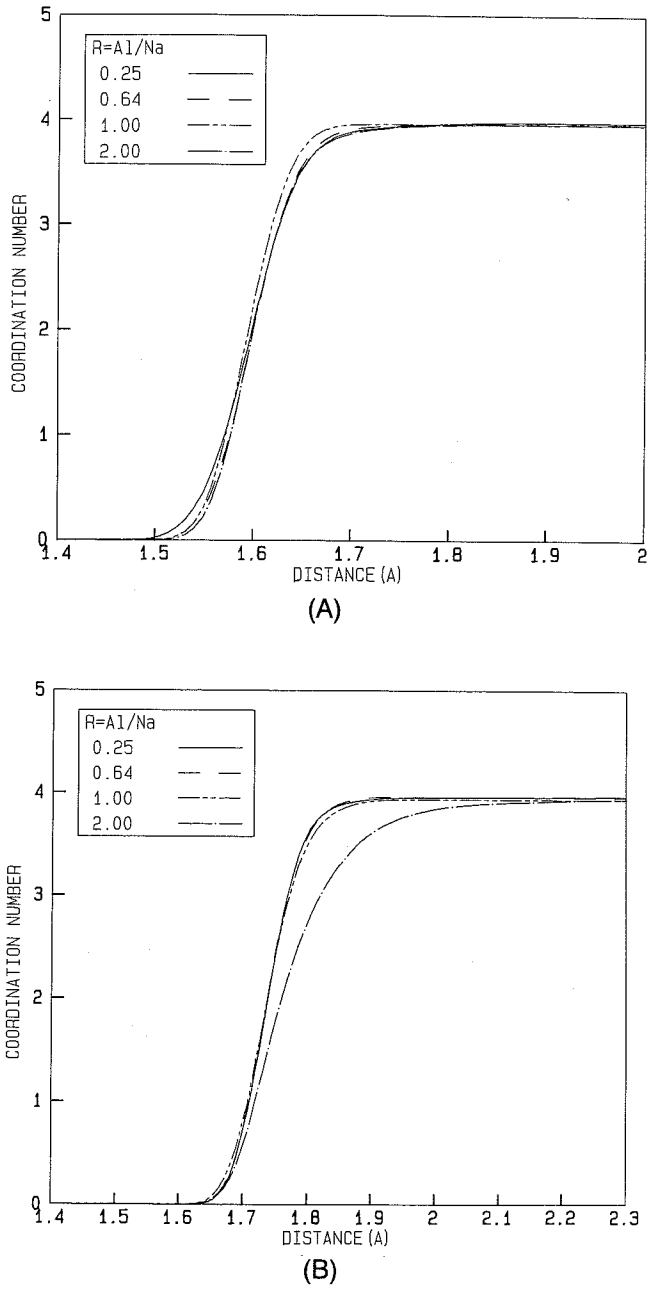

Fig. 2. Coordination of oxygen plotted versus distance around (A) Si and (B) Al.

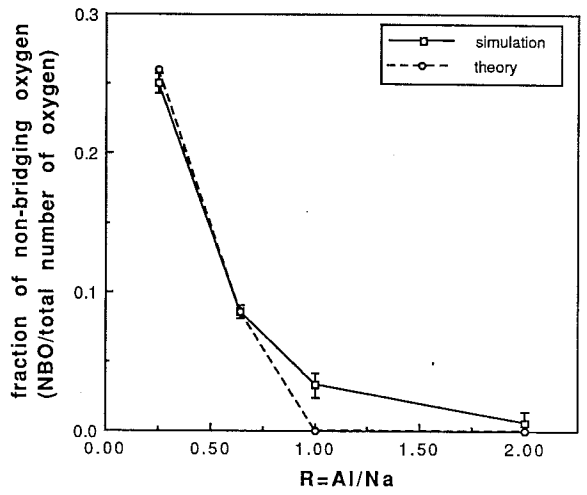

Fig. 3. Concentration of nonbridging oxygen plotted versus composition: (solid curve) simulations, (dashed curve) theory (see Ref. 37.)

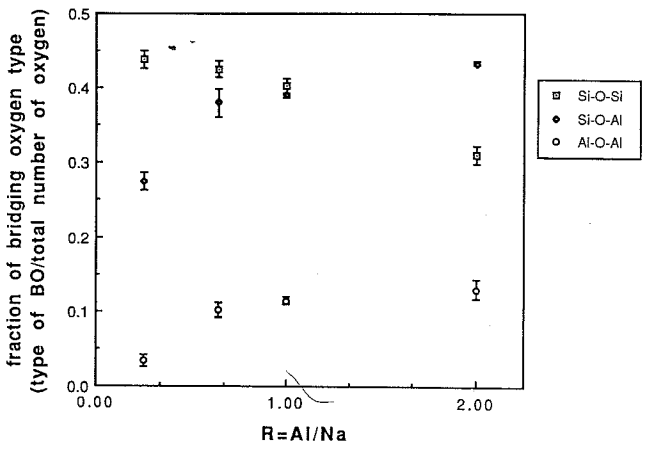

Fig. 4. Types of bridging oxygen plotted versus composition.

Al. Al–O–Al linkages are thought to be unlikely because of their inherent electrostatic instability, since Pauling's second rule predicts a bond strength of 1.5 on the BO and thus the BO is associated with too many electrons.[39,40] MAS-NMR (magic angle spinning nuclear magnetic resonance) has been used to distinguish between occupancy of tetrahedral sites based upon ^{29}Si shifts. These shifts were attributed to the degree of condensation of silicate tetrahedra and to the substitution of aluminum for silicon in the tetrahedral sites. ^{29}Si MAS-NMR performed on a Linde-A zeolite (aluminosilicate-cage-like structure) contradicts Lowenstein's principle since the structure consists of a 3:1 ordering of Si:Al.[39] The 3:1 ordering implies that every silicon tetrahedron was surrounded by three aluminate tetrahedra and one silicate tetrahedron and every aluminate tetrahedron was surrounded by three silicate tetrahedra and one aluminate tetrahedron. Therefore, Al–O–Al bonds must have been present in the zeolitic structure. The open structure of the zeolites absorbs much of the strain associated with the Al–O–Al linkages. Because of the open ringlike structure of the NAS glasses, similar arguments may therefore be made for the presence of Al–O–Al linkages in NAS glasses.

Triclusters were present in compositions with $R \geq 1$. These were oxygens which were bonded to three cations (Si and/or Al) as they sat at the vertex of three tetrahedra. The concentration of triclusters versus glass composition (R) is shown in Fig. 5. The total concentration compares favorably with Lacy's[9] proposition that triclusters are present in the glasses based upon geometric and packing arguments. The specific types of triclusters (number of different types of cations) present are shown in Fig. 6. As the glass composition approached $R = 2$, higher concentrations of triclusters containing three aluminate and no silicate tetrahedra (3Al–0Si) and two aluminate and one silicate tetrahedra (2Al–1Si) were formed, indicating that the glasses may have begun to separate into silica-rich and aluminate-rich regions.

The inverse relationship between the concentration of NBO and triclusters has been shown in earlier simulations of NAS glasses[28] using only two-body interatomic potentials. The concentration of NBO for glasses with $R \geq 1$ was fairly constant at about 10% in the simulations using only pair potentials, while the concentration of triclusters was about 10% for glasses with $R = 1.0$ and 35% for glasses with $R = 2.0$ (compare to multibody results in Figs. 3 and 6).

The role of sodium in the NAS glasses was either to act as a network modifier and coordinate the NBO or to act as a charge compensator for the $[AlO_4]^-$ tetrahedra and coordinate the BO associated with the Al. The coordination of the sodium at specific types of bridging and nonbridging oxygens in the simulations is presented in Fig. 7. The coordination

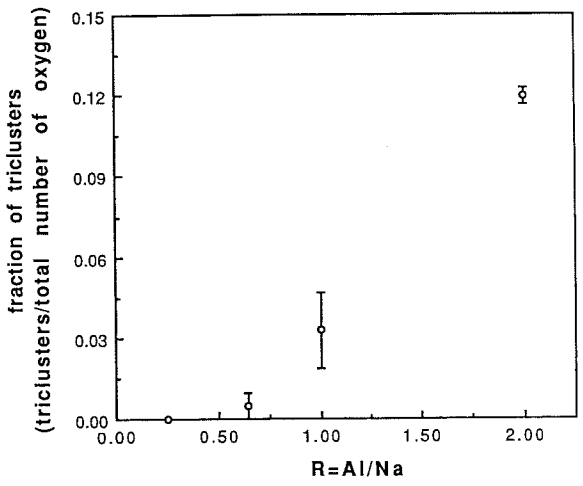

Fig. 5. Concentration of triclusters plotted versus composition.

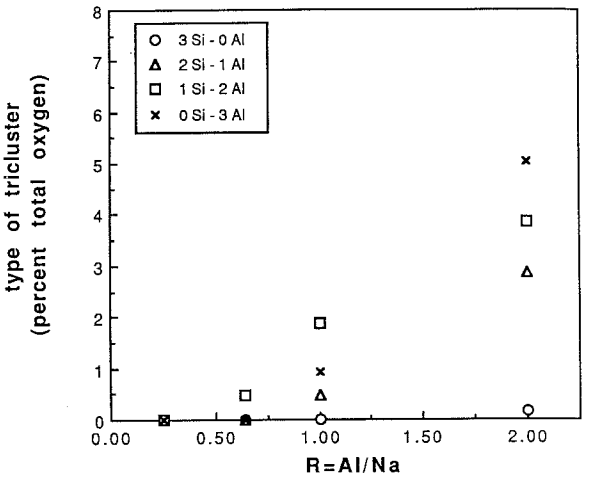

Fig. 6. Types of tricluste · plotted versus composition.

numbers were found from the area under the individual PDFs and from coordination distance curves like those shown in Fig. 2 for Si and Al. The Na–O bond length was approximately 2.4 to 2.6 Å, which compares favorably with bond lengths derived from EXAFS analysis[10b] and prior simulations on silicate glasses.[28,41]

In glasses with compositions of $R \leq 1$, Na was associated in high concentrations both at the NBO sites and at oxygen associated with aluminate tetrahedra (at Al–O–Al and Si–O–Al sites). In compositions with $R = 2$ the sodium was found at aluminate and silicate tetrahedra. Thus the role of sodium changes from being both a network modifier and charge compensator to being only a charge compensator. Note that no sodium was associated with the triclusters. The simulations, therefore, effectively reproduced the structural roles of the sodium.[42]

(2) Network Connectivity

Medium-range order in glasses was characterized by the distribution of various-sized rings within the glass network. A ring was considered to be the shortest set of (n) X–O bonds over which a closed path exists, where X is any network-forming cation (Si or Al) and n goes from $n = 2$ to $n > 8$. The ring size distribution for the series of NAS glasses is presented in Fig. 8(A) and the average ring size for each glass is shown in Fig. 8(B). Increasing the ratio of Al/Na caused a decrease in the average ring size from about 5.8 for glasses

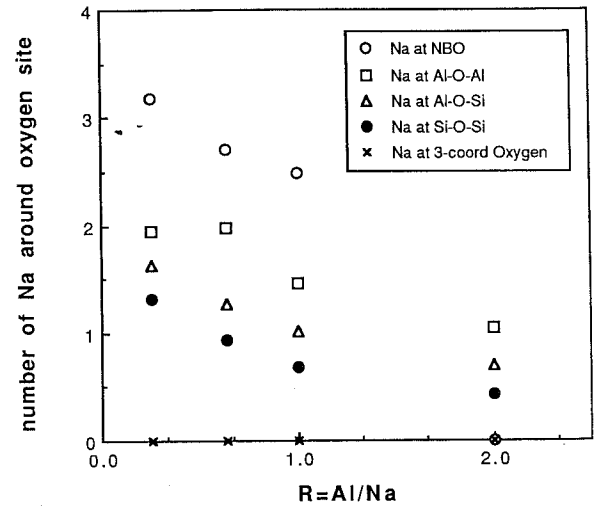

Fig. 7. Coordination of sodium at various types of oxygen plotted versus composition. Coordination within 3.5 Å of oxygen.

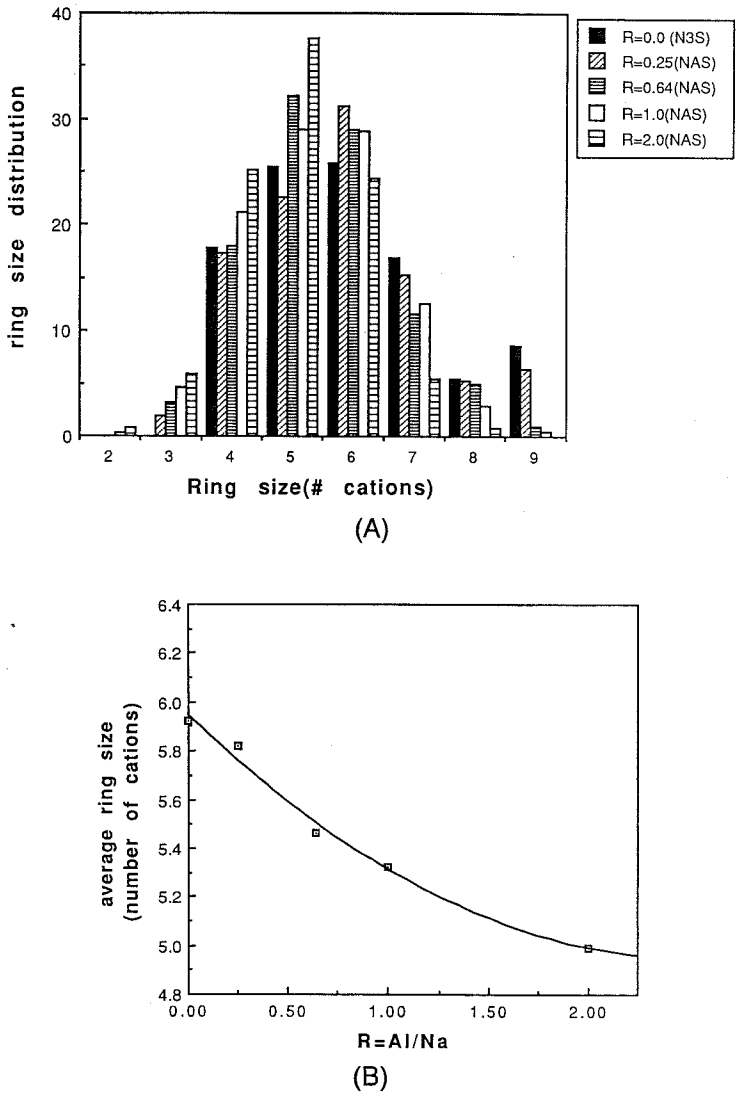

Fig. 8. (A) Ring size distribution and (B) average ring size for NAS and sodium trisilicate glasses.

with compositions of $R = 0.25$ to about 5 for glasses with compositions of $R = 2$. The larger rings (>8) associated with the glasses with compositions of $R = 0.25$ were due to the high concentration of NBO which caused many rings not to close and left the glass network consisting of large channels. This type of structure has been observed for the sodium silicate glasses, $Na_2O \cdot 3SiO_2$ (N3S), where the "open" structure leads to the high diffusivity of sodium through the sodium trisilicate network.[13,28–31,41,43] Sodium silicates are precursor glasses to the NAS series as they can be considered to be NAS glasses with compositions of $R = 0$. The ring size distribution and average ring size (≈5.9) for the N3S glass are included in Figs. 8(A) and (B).

The rings in the N3S glasses were composed of only Si cations,[43] but rings in the NAS glasses contained Si and Al cations. As Al was incorporated into the glass composition (R was increased), some of the Si rings in N3S had to be replaced with the Si–Al type of rings.

The number of each type of cation in the three-, four-, and five-membered rings was determined as a function of the glass composition in order to ascertain if there was preferential replacement of Si by Al in any of the rings. The probability of Al being in a ring was compared to the actual percent of Al in the ring to determine if there was preferential replacement of the Si. Figure 9 presents the fraction of Si in each of the three-, four-, and five-membered rings along with the theoretical fraction of Si that should be in the ring if there was uniform replacement of the Si by Al.[44] There is good agreement between the theoretical and simulated curves, such that Al was randomly incorporated into the four- and five-membered rings (Figs. 9(B) and 9(C)); however, there was preferential replacement of the Al in the three-membered rings (Fig. 9(A)) since the simulated curve is substantially less than the theoretical curve.

(3) Macroscopic Properties

Figure 10 shows an example of the mean squared displacement of the sodium atoms plotted versus time (Eq. (4)) for a composition with $R = 0.25$ at temperatures of 6500, 6000, 5000, and 4000 K. These temperatures correspond to approximately $2.2T_g$, $2.0T_g$, $1.6T_g$, and $1.3T_g$, where T_g is the glass transition temperature and had a value of approximately 3000 K for the simulated glasses. The slopes of the curves in Fig. 10 (and similar curves for the other three compositions) were used in determining the diffusion coefficients via Eq. (5), from which the activation energies for diffusion for each composition were computed using Eq. (6). The activation energies for sodium diffusivity plotted versus composition are presented in Fig. 11. Assuming that electrical conductivity occurs in NAS glasses via Na diffusion, then the minimum which occurred in the activation energy for the glasses with compositions of $R = 1.0$ correspond to the minimum observed in the measurements of activation energy for electrical conductivity.[1,4,6,7,45,46]

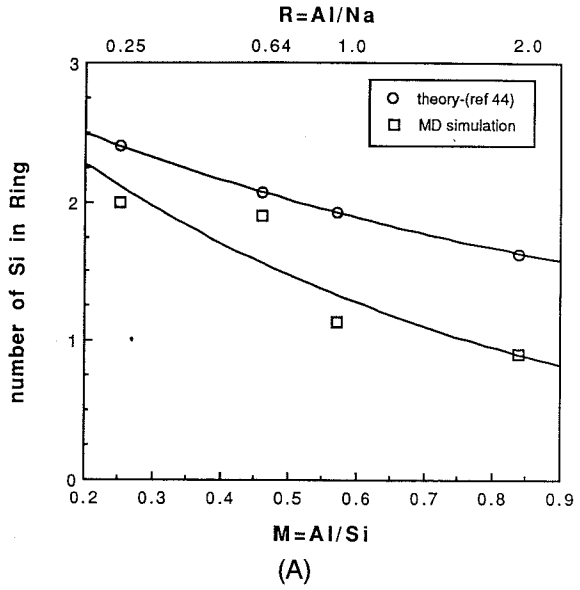

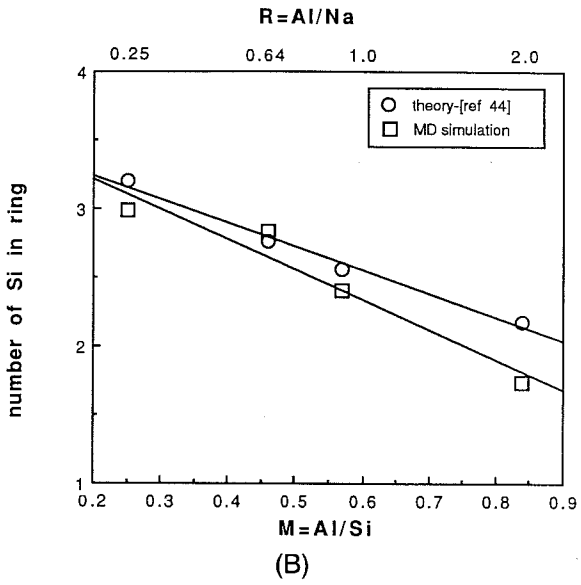

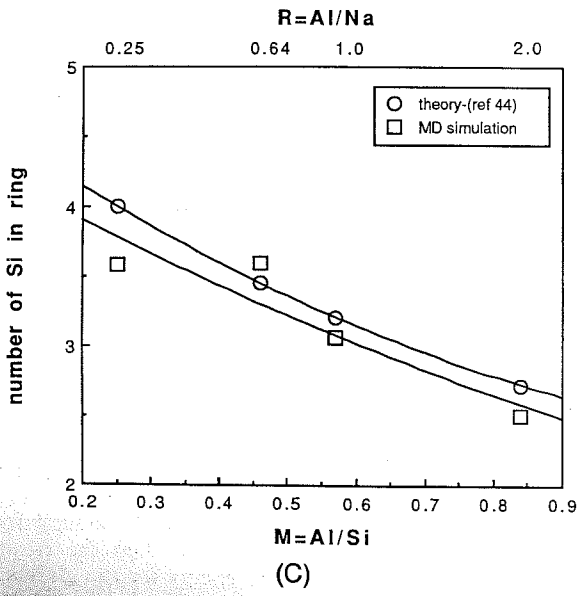

Fig. 9. Distribution of cations in rings (number of Si per ring) for (A) three-membered rings, (B) four-membered rings, and (C) five-membered rings.

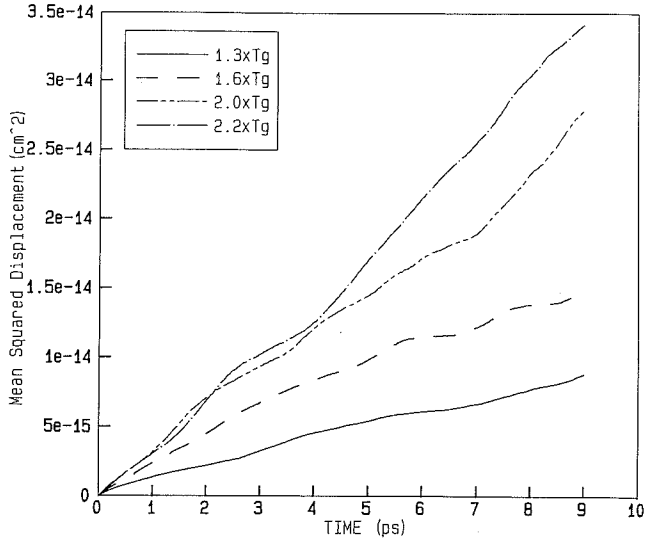

Fig. 10. Mean squared displacement plotted versus composition for glass with composition of $R = 0.25$ at temperatures of $2.2T_g$, $2T_g$, $1.6T_g$, and $1.3T_g$.

Diffusion of Na was a multistep process. The first step involved breaking Na–O bonds and the second step involved sodium diffusing to new energetically favorable binding sites. In glasses with compositions of $R < 1$, sodium ions were predominantly bonded to NBO. Diffusion of the sodium occurred as Na–NBO bonds were broken and sodium hopped between NBO sites within the large open channels that were discussed in Section III(2). The activation energy for diffusion was high for compositions with $R < 1$ as it was difficult to break the Na–NBO bonds. In an earlier simulation of alkali adsorption onto silica surfaces,[48] the alkali–NBO bond was shown to be "effectively" stronger because of greater contributions from Coulombic interactions caused by a shorter alkali–NBO bond length in comparison to the alkali–BO bond length. Given sufficient kinetic energy to overcome a Na–NBO bond in the glasses with $R < 1$, Na diffused to other NBO sites within the large channels in the glasses. At $R = 1$, the concentration of Al was increased, such that there were fewer NBOs in the system and more Na were associated with aluminate tetrahedra than with NBO. The activation energy for diffusion decreased as it became easier to break Na–BO bonds as opposed to Na–NBO bonds.

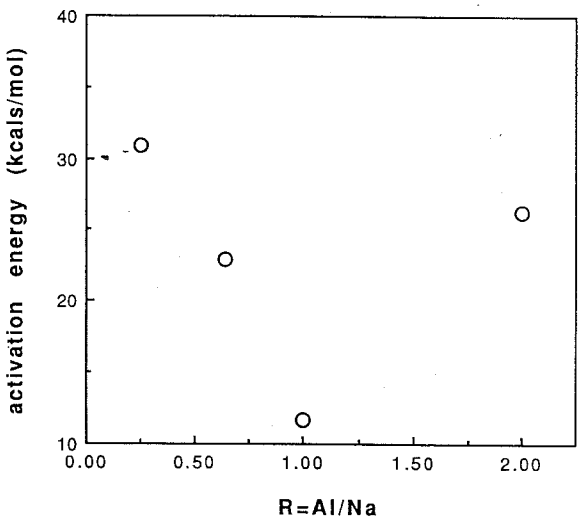

Fig. 11. Sodium activation energy for diffusion versus glass composition.

In glasses with compositions of $R = 2$, the Na–BO bonds were of the same strength as they were in glasses with compositions of $R = 1$. However, the activation energy for diffusion increased because of the presence of triclusters and the elimination of the large NBO-lined channels. Given sufficient thermal energy the Na–BO bond could be broken in the glasses with compositions of $R = 2$, but the increased concentration of triclusters reduced the availability of energetically favorable binding sites such that there were large activation barriers to Na diffusion. The reduction in the concentration of energetically favorable sites can be noted in Fig. 7, where no Na was associated with either NBO or triclusters in glasses with compositions of $R = 2$. The activation barriers were associated with the increased distance that Na had to diffuse in order to find more favorable bonding sites.

The diffusion coefficients for all of the species in the glasses were determined in a similar manner as was used to determine those for just sodium and are plotted in Fig. 12 at temperatures of $2T_g$ and $1.6T_g$. From the inverse relationship between viscosity and diffusivity, the minimum in diffusivity (at the composition with $R = 1.0$ in Fig. 12) corresponds to the experimentally measured maximum in the viscosity of the glasses at $R = 1.0$.[5,7,47] The decrease in the diffusivity of all of the species (see Fig. 12) as aluminum was substituted for sodium up to the equivalence point can be attributed to the reduction in the NBO concentration as well as to the cross-linking of Al–O bonds across channels. In glasses with compositions of $R > 1$, the diffusion rates increased and the "viscosity" decreased because of the presence of the triclusters. The triclusters were more easily rearranged in response to the increased temperature than were the two-coordinated bridging oxygen since the bonds associated with the triclusters (three-coordinated bridging) were longer than those associated with the two-coordinated bridging oxygen (see long tails in Figs. 1(A) and (B) for $R = 2.0$ glasses). The longer Si–O or Al–O bonds associated with the triclusters were easier to break and thus created bond defects which were similar to the NBO in the N3S glasses that allowed for atomic rearrangement.

IV. Summary

The relationships between atomic structure and physically observable properties have been studied for a series of NAS glasses. The MD technique was used to model NAS glasses with a tetrahedral form of a multibody potential applied to Si, O, and Al atoms. Local bonding environments within the glass network compared favorably with experimentally derived bond lengths, and coordination numbers. The resulting glasses exhibited extrema in the diffusion coefficients for all of the species and in the activation energy for sodium diffusion which corresponded with extrema observed in the viscosity and in the activation energies for electrical conductivity. The changes in the physical properties were found to correspond with (1) the reduction in the concentration of nonbridging oxygen as the compositions of the glasses passed through the equivalence point in the ratio (R) of Al_2O_3 to Na_2O, (2) the introduction of oxygen triclusters as the ratio (R) became greater than 1, and (3) the elimination of large rings associated with glasses with low aluminum concentration which led to an overall reduction in the ring size distribution within the glass networks. Aluminum coordination remained 4 over the entire compositional range; thus there was no need to invoke a change in aluminum coordination as an explanation for the changes in the physical properties.

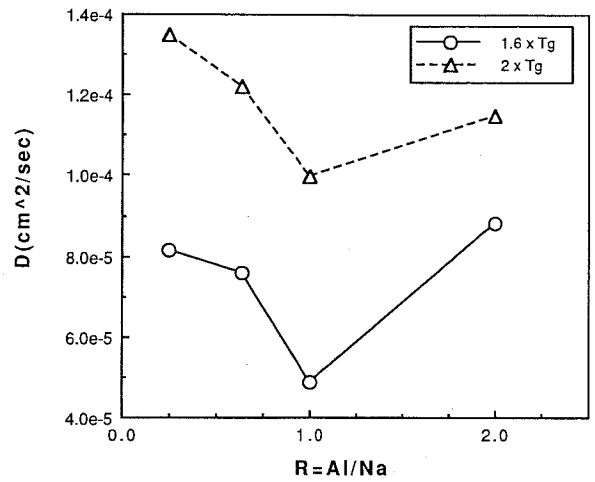

Fig. 12. Diffusivity for all species versus composition at $2T_g$ and $1.6T_g$.

References

[1]J. O. Isard, "Electrical Conductivity in Aluminosilicate Glasses," *J. Soc. Glass Technol.*, **43** [211] 113–23 (1959).

[2]H. Moore and P.W. McMillan, "A Study of Glasses Consisting of the Oxides of Elements of Low Atomic Weight. Part II. The Absorption Characteristics of Certain of the Experimental Glasses," *J. Soc. Glass Technol.*, **40**, 97–138 (1956).

[3](a) D. E. Day and G. E. Rindone, "Properties of Soda Aluminosilicate Glasses: I, Refractive Index, Density, Molar Refractivity, and Infrared Absorption Spectra," *J. Am. Ceram. Soc.*, **45** [10] 489–96 (1962). (b) D. E. Day and G. E. Rindone, "Properties of Soda Aluminosilicate Glasses: II, Internal Friction," *ibid.*, **45** [10] 496–504 (1962). (c) D. E. Day and G. E. Rindone, "Properties of Soda Aluminosilicate Glasses: III, Coordination of Aluminum Ions," *ibid.*, **45** [12] 579–81 (1962). (d) P.W. L. Graham and G. E. Rindone, "Properties of Soda Aluminosilicate Glasses: IV, Relative Acidities and Some Thermodynamic Properties," *ibid.*, **47** [1] 19–24 (1964). (e) T. D. Taylor and G. E. Rindone, "Properties of Soda Aluminosilicate Glasses: V, Low-Temperature Viscosities," *ibid.*, **53** [12] 692–95 (1970).

[4]E. L. Williams and R.W. Heckman, "Sodium Diffusion in Soda–Lime–Aluminosilicate Glasses," *Phys. Chem. Glasses.*, **5** [6] 166–71 (1964).

[5]E. F. Riebling, "Structure of Sodium Aluminosilicate Melts Containing at Least 50 mol% SiO_2 at 1500°C," *J. Chem. Phys.*, **44** [8] 2857–65 (1966).

[6]R. Terai, "Self-Diffusion of Sodium Ions and Electrical Conductivity in Sodium Aluminosilicate Glasses," *Phys. Chem. Glasses*, **10** [4] 146–52 (1969).

[7]K. Hunold and R. Brückner, "Physikalische Eigenschaften und Strukturelle Feinbau von Natrium-Aluminosilicateglasern und -Schmelzen," *Glastech. Ber.*, **53**, 149–61 (1980).

[8]A. Klonkowski, "The Structure of Sodium Aluminosilicate Glass," *Phys. Chem. Glasses*, **24** [6] 166–71 (1983).

[9]E. D. Lacy, "Aluminum in Glasses and in Melts," *Phys. Chem. Glasses*, **4** [6] 234–38 (1963).

[10](a) D. A. McKeown, F. L. Galeener, and G. E. Brown, "Raman Studies of Al Coordination in Silica-Rich Sodium Aluminosilicate Glasses and Some Related Minerals," *J. Non-Cryst. Solids*, **68**, 361–78 (1984). (b) D. A. McKeown, G. A. Waychunas, and G. E. Brown, "EXAFS and XANES Study of the Local Coordination Environment of Sodium in a Series of Silica Rich Glasses and Selected Minerals within the Na_2O–Al_2O_3–SiO_2 System," *ibid.*, **74**, 325–48 (1985). (c) D. A. McKeown, G. A. Waychunas, and G. E. Brown, "EXAFS Study of the Coordination Environment of Aluminum in a Series of Silica Rich Glasses and Selected Minerals within the Na_2O–Al_2O_3–SiO_2 System," *ibid.*, **74**, 349 (1985). (d) D. A. McKeown, "Radial Distribution Analysis of a Series of Silica Rich Sodium Aluminosilicate Glasses Using Energy Dispersive X-ray Diffraction," *Phys. Chem. Glasses*, **28** [4] 156–63 (1987).

[11]G. Engelhardt, M. Nofz, K. Forkel, F. G. Wihsmann, M. Magi, A. Samoson, and E. Lippmaa, "Structural Studies of Calcium Aluminosilicate Glasses by High Resolution Solid State ^{29}Si and ^{27}Al Magic Angle Spinning Nuclear Magnetic Resonance," *Phys. Chem. Glasses*, **26** [5] 157–65 (1985).

[12]T. Hanada, T. Aikawa, and N. Soga, "Coordination of Aluminum in Amorphous Sodium Aluminosilicate Films," *J. Non-Cryst. Solids*, **50**, 397–405 (1982).

[13]C. A. Angell, P. Cheeseman, and S. Tamaddon, "Pressure Enhancement of Ion Mobilities in Liquid Silicates from Computer Simulation Studies to 800 kilobars," *Science*, **218**, 885–87 (1982).

[14]E. Ohtani, F. Taulelle, and C. A. Angell, "Al^{3+} Coordination Changes in Liquid Aluminosilicates under Pressure," *Nature (London)*, **314**, 78–81 (1985).

[15]R. Brückner, H. U. Chun, and H. Goretzki, "Photoelectron Spectroscopy (ESCA) on Alkali Silicate and Soda Aluminosilicate Glasses," *Glastech. Ber.*, **51** [1] 1–7 (1978).

[16]B. M. J. Smets and T. P. A. Lommen, "The Incorporation of Aluminum Oxide and Boron Oxide in Sodium Silicate Glasses, Studied by X-ray Photoelectron Spectroscopy," *Phys. Chem. Glasses*, **22** [6] 158–62 (1981).

[17]D. J. Lam, A. P. Paulikas, and B.W. Veal, "X-ray photoemission Spectroscopic Studies of Soda Aluminosilicate Glasses," *J. Non-Cryst. Solids*, **42**, 41–48 (1980).

[18]Y. Kaneko, H. Nakamura, M. Yamane, K. Mizoguchi, and Y. Suginohara, "Photoelectron Spectra of Silicate Glasses Containing Trivalent Cations," *Yogyo Kyokaishi*, **91** [7] 321–24 (1983).

[19]P. I. K. Onorato, M. N. Alexander, C.W. Struck, G.W. Tasker, and D. R. Uhlmann, "Bridging and Nonbridging Oxygen Atoms in Alkali Aluminosilicate Glasses," *J. Am. Ceram. Soc.,* **68** [6] C-148–C-150 (1985).

[20]G.W. Tasker, D. R. Uhlmann, P. I. K. Onorato, M. M. Alexander, and C.W. Struck, "Structure of Sodium Aluminosilicate Glasses: X-ray Photoelectron Spectroscopy," *J. Phys. (Orsay, Fr.) C8,* **12** [46] 273–80 (1985).

[21]P. I. K. Onorato, M. M. Alexander, C.W. Struck, G.W. Tasker, and D. R. Uhlmann, "Structure of Sodium Aluminosilicate Glasses: Tl Luminescence Spectroscopy," *J. Phys. (Orsay, Fr.) C8,* **12** [46] 235–40 (1985).

[22]M. N. Alexander, P. I. K. Onorato, C.W. Struck, J. R. Rozen, G.W. Tasker, and D. R. Uhlmann, "Structure of Alkali(Alumino)Silicate Glasses: I. Tl^+ Luminescence and the Nonbridging Oxygen Issue," *J. Non-Cryst. Solids,* **79**, 137–54 (1986).

[23]M. N. Alexander, P. I. K. Onorato, C.W. Struck, G.W. Tasker, and D. R. Uhlmann, "Structure of Alkali(Alumino) Silicate Glasses: II. Luminescence of Thallium-Doped Sodium Aluminosilicates and Implications for Optical Basicity Theories," *J. Non-Cryst. Solids,* **91**, 63–82 (1987).

[24]S. H. Garofalini, "Molecular Dynamics Simulation of the Frequency Spectrum of Amorphous Silica," *J. Chem. Phys.,* **76**, 3189 (1982).

[25]B. P. Feuston and S. H. Garofalini, "Empirical Three-Body Potential for Vitreous Silica," *J. Chem. Phys.,* **89** [9] 5818–24 (1988).

[26]R. G. Newell, B. P. Feuston, and S. H. Garofalini, "The Structure of Sodium Trisilicate Glass via Molecular Dynamics Employing Three-Body Potentials," *J. Mater. Res.,* **4** [2] 434–439 (1989).

[27]Q_i species are defined as the number of bridging oxygens around a network-forming cation. For example, Q_3 means that there are three bridging oxygens and one nonbridging oxygen around a silicon.

[28]T. J. Soules, "Molecular Dynamic Calculations of Glass Structure and Diffusion," *J. Non-Cryst. Solids,* **49**, 29–52 (1982).

[29]C. A. Angell, P. Cheesesman, and S. Tamaddon, "Computer Simulations Studies of Migration Mechanisms in Ionic Glasses and Liquids," *J. Phys. (Orsay, Fr.), C9,* **12** [43] 381–85 (1982).

[30]C. A. Angell, P. Cheesesman, and S. Tamaddon, "Water-like Transport Property Anomalies in Liquid Silicates Investigated at High T and P by Computer Simulation Techniques," *Bull. Mineral.,* **106**, 87–97 (1983).

[31]S. H. Garofalini and S. Conover, "Comparison between Bulk and Surface Self-Diffusion Constants of Si and O in Vitreous Silica," *J. Non-Cryst. Solids,* **74**, 171–76 (1985).

[32](a) A. Nordsieck, "On Numerical Integration of Ordinary Differential Equations," *Math. Comput.,* **16**, 22 (1962). (b) C.W. Gear, The Numerical Integration of Ordinary Differential Equations of Various Orders, ANL 7126, Argonne National Laboratory Report, 1966.

[33]F. H. Stillinger and T. A. Weber, "Computer Simulation of Local Order in Condensed Phases of Silicon," *Phys. Rev. B,* **31**, 5262–71 (1985).

[34]M. Taylor and G. E. Brown, Jr., "Structure of Mineral Glasses—I. The Feldspar Glasses $NaAlSi_3O_8$, $KAlSi_3O_8$, $CaAl_2O_8$," *Geochim. Cosmochim. Acta,* **43**, 61–75 (1979).

[35]J.V. Smith, G. Artioli, and A. Kvick, "Low Albite, $NaAl_3SiO_8$: Neutron Diffraction Study of Crystal Structure," *Am. Mineral.,* **71**, 727–33 (1986).

[36]A. Navrotsky, K. L. Geisinger, P. McMillan, and G.V. Gibbs, "The Tetrahedral Framework in Glasses and Melts—Inferences from Molecular Orbital Calculations and Implication for Structure, Thermodynamics and Physical Properties," *Phys. Chem. Miner.,* **11**, 284–98 (1985).

[37]Fraction of NBO = $[2X_{Na} - 2X_{Al}]/[X_{Na} + 3X_{Al} + 2X_{Si}]$, where X is the mole fraction of Na_2O, Al_2O_3, and SiO_2, respectively (Ref. 18).

[38]W. Lowenstein, "The Distribution of Aluminum in the Tetrahedra of Silicates and Aluminates," *Am. Mineral.,* **39**, 92–96 (1954).

[39]J. Klinowski, J. M. Thomas, C. A. Fyfe, and J. S. Hartman, "Applications of Magic-Angle-Spinning Silicon-29 Nuclear Magnetic Resonance. Evidence for Two Different Kinds of Silicon–Aluminum Ordering in Zeolitic Structures," *J. Phys. Chem.,* **85**, 2590–94 (1981).

[40]B. H.W. S. De Jong, C. M. Schramm, and V. E. Parziale, "Polymerization of Silicate and Aluminate Tetrahedra in Glasses, Melts, and Aqueous Solutions —IV. Aluminum Coordination in Glasses and Aqueous Solutions and Comments on the Aluminum Avoidance Principle," *Geochim. Cosmochim. Acta,* **47**, 1223–36 (1983).

[41]S. K. Mitra and R.W. Hockney, "Microheterogeneity in Simulated Soda Silica Glass"; pp. 316–25 in The Structure of Non-Crystalline Materials. Edited by P. H. Gaskell, J. M. Parker, and E. A. Davis. Taylor and Francis, New York, 1982.

[42]N. J. Kreidl, "Inorganic Glass-Forming Systems; pp. 105–90 in Glass: Science and Technology, Vol. 1, Glass Forming Systems. Edited by D. R. Uhlmann and N. J. Kreidl. Academic Press, New York, 1983.

[43]H. S. Melman and S. H. Garofalini, "Microstructural Evaluation of Simulated Sodium Silicate Glasses"; unpublished work.

[44]For example, if there were random replacement of Al for the Si in the three-membered rings for the $R = 0.25$ glasses, then the ratio (M) of Al/Si would be $M = 0.25$ (see Table III) yielding 0.2 Al per 0.8 Si. The average three-membered ring would therefore contain 3×0.2 Al and 3×0.8 Si or 0.6 Al and 2.4 Si.

[45]H. Wakabayashi, "The Relationship between Composition and Electrical Conductivity in Glasses Containing Network Forming Trivalent Cations," *Phys. Chem. Glasses,* **30** [2] 51–54 (1989).

[46]G. J. Frischat, Ionic Diffusion in Oxide Glasses; Vol. 3/4 in Diffusion and Defect Monograph Series. Edited by Y. Adda, A. D. LeClaire, L. M. Slifkin, and F. H. Wohlbier. Trans Tech Publ., Bay Village, OH, 1975.

[47]R. Brückner, "Structure and Properties of Silicate Melts," *Bull. Mineral.,* **106**, 9–22 (1983).

[48]S. H. Garofalini and D. M. Zirl, "Onset of Alkali Adsorption on the Vitreous Silica Surface," *J. Vac. Sci. Technol. A.,* **6** [3] 975–81 (1988). □